Lightning Frequency and Microphysical Properties of Precipitating Clouds over the Western North Pacific during Winter as Derived from TRMM Multisensor Observations

YASU-MASA KODAMA, HARUNA OKABE, YUKIE TOMISAKA, KATSUYA KOTONO,* YOSHIMI KONDO,+ AND HIDEYUKI KASUYA#

Department of Earth and Environmental Sciences, Hirosaki University, Hirosaki, Aomori, Japan

(Manuscript received 23 August 2005, in final form 6 September 2006)

ABSTRACT

Tropical Rainfall Measuring Mission observations from multiple sensors including precipitation radar, microwave and infrared radiometers, and a lightning sensor were used to describe precipitation, lightning frequency, and microphysical properties of precipitating clouds over the midlatitude ocean. Precipitation over midlatitude oceans was intense during winter and was often accompanied by frequent lightning. Case studies over the western North Pacific from January and February 2000 showed that some lightning occurred in deep precipitating clouds that developed around cyclones and their attendant fronts. Lightning also occurred in convective clouds that developed in regions of large-scale subsidence behind extratropical cyclones where cold polar air masses were strongly heated and moistened from below by the ocean. The relationships between lightning frequency and the minimum polarization corrected temperature (PCT) at 37 and 85 GHz and the profile of the maximum radar reflectivity resembled relationships derived previously for cases in the Tropics. Smaller lapse rates in the maximum radar reflectivity above the melting level indicate vigorous convection that, although shallow and relatively rare, was as strong as convection over tropical oceans. Lightning was most frequent in systems for which the minimum PCT at 37 GHz was less than 260 K. Lightning and PCT at 85 GHz were not as well correlated as lightning and PCT at 37 GHz. Thus, lightning was frequent in convective clouds that contained many large hydrometeors in the mixed-phase layer, because PCT is more sensitive to large hydrometeors at 37 than at 85 GHz. The relationship between lightning occurrence and cloud-top heights derived from infrared observations was not straightforward. Microphysical conditions that support lightning over the midlatitude ocean in winter were similar to conditions in the Tropics and are consistent with Takahashi's theory of riming electrification.

1. Introduction

The Tropical Rainfall Measuring Mission (TRMM) satellite carries a precipitation radar (PR; Iguchi et al. 2000), a Visible and Infrared Scanner (VIRS), the TRMM Microwave Imager (TMI; Kummerow et al. 1998, 2000), and a Lightning Imaging Sensor (LIS; Christian et al. 1999) and therefore can perform satellite-based multisensor observations of precipitation. Multisensor observations from TRMM can evaluate microphysical features and internal structures in precipitating clouds. LIS lightning observations combined with microphysical observations yield useful information about cloud electrification mechanisms. Lightning occurrence depends on microphysical conditions in the mixed-phase layer (MPL) of clouds that favor charge separation. Laboratory experiments (Takahashi 1978, 1985; Saunders et al. 1991) and numerical experiments (Takahashi 1983, 1984) suggest that such cloud conditions include abundant amounts of small ice, large graupel, and supercooled cloud water in the MPL.

Toracinta et al. (1996) analyzed several mesoscale convective systems over Texas observed by ground-based instruments and noted that frequent lightning was often accompanied by reflectivities exceeding 35

* Current affiliation: NTT DATA Creation Corporation, Tokyo, Japan.
+ Current affiliation: Iwai High School, Bando, Ibaraki, Japan.
# Current affiliation: Fujitsu FIP Co., Tokyo, Japan.

Corresponding author address: Yasu-Masa Kodama, Department of Earth and Environmental Sciences, Hirosaki University, 3 Bunkyo-cho, Hirosaki, Aomori 036-8561, Japan.
E-mail: kodama@cc.hirosaki-u.ac.jp

DOI: 10.1175/MWR3388.1

dBZ and a small lapse rate in reflectivity in the MPL. Cecil and Zipser (2002) compared TRMM-PR and LIS observations for many precipitation features in the Tropics and found a relationship between radar reflectivity and lightning that is similar to that reported by Toracinta et al. (1996).

Results from Zipser and Lutz (1994) and Toracinta et al. (1996) suggest that radar reflectivity above the melting level (ML) is sensitive to large hydrometeors (i.e., large graupel, hail, and large supercooled raindrops) in the Rayleigh regime, when the size of hydrometeors is much smaller than the wavelength. Large reflectivity and a small lapse late in reflectivity above the ML thus indicate vigorous convection, because such reflectivity features occur when large hydrometeors are suspended above the ML by a strong updraft in the deep convective clouds. In addition, Cecil and Zipser (2002) outlined a conceptual model in which echo tops of 20–30 dBZ (greater than 30 dBZ) approximately correspond to the upper limit of small precipitation-size graupel (large graupel).

The brightness temperatures (TBBs) at 37 and 85 GHz also yield information on cloud physics related to lightning frequency. In rainfall areas, upwelling emissions at the ML (i.e., at the top of a liquid-phase layer) are saturated in these channels of the TMI, especially at 85 GHz, when the optical thickness of the liquid-phase layer is large. In such cases, upwelling radiation at the ML is almost independent of both liquid water content in the layer and ground surface radiation. The upwelling radiation is attenuated above the ML by scattering by precipitation-size ice particles and large raindrops in the MPL (Wu and Weinman 1984; Wilheit 1986; Spencer 1986). Over the ocean, observations of cooler TBB unrelated to scattering occur because of the low emissivity of the water surface. Spencer et al. (1989) introduced the polarization-corrected temperature (PCT) that is a linear function of TBBs observed in the horizontal and vertical polarization channels. The PCT shows the intensity of scattering after the influence of radiation from the underlying surface is minimized. PCT37 and PCT85 in this study refer to PCTs at 37 and 85 GHz, respectively, which are used to evaluate scattering intensity. PCTs were derived from TMI TBB in the horizontal (suffix h) and vertical (suffix v) polarization channels at 85 and 37 GHz as follows:

$$\mathrm{PCT85} = 1.82\mathrm{TBB85v} - 0.82\mathrm{TBB85h}$$
(after Spencer et al. 1989)

and

$$\mathrm{PCT37} = 2.20\mathrm{TBB37v} - 1.20\mathrm{TBB37h}$$
(after Cecil et al. 2002).

Lower PCT values indicate stronger scattering. PCT85 is more sensitive to relatively small precipitation-size ice particles in the upper part of clouds and PCT37 is more sensitive to large frozen or supercooled hydrometeors, such as large graupel, large supercooled water droplets, and large aggregated snowflakes, just above the ML (Wu and Weinman 1984; Adler et al. 1991; Cecil and Zipser 2002). A lower PCT37 therefore indicates vigorous convection with strong updrafts that sustain the larger hydrometeors (Cecil and Zipser 2002), except for cases in which the hydrometeor size is comparable to the wavelength (i.e., in the Mie regime). Scattering efficiency for such cases can oscillate in a behavior that differs at 85 and 37 GHz, and PCT85 and PCT37 are highly sensitive to the drop size distribution. Nonuniform beamfilling effects also exist when the TMI channel footprint is partially cloud covered (Spencer 1986), and the observed TBB is consequently a mixture of TBBs from the cloud and earth surfaces. The observed TBB for such cases can differ greatly from the true cloud-only TBB. Nonuniform beamfilling effects for small clouds are greater at 37 GHz because the footprint size is larger than at 85 GHz.

Emissions also contribute to the PCTs. For example, upwelling radiation may be augmented in a MPL because supercooled cloud water that coexists with precipitation-size ice particles in the scattering layer can increase the PCT, especially at 85 GHz (Vivekanandan et al. 1991; Toracinta et al. 2002; Smith et al. 1992; Adler et al. 1991; Cecil and Zipser 2002). In addition, the saturation hypothesis at the ML becomes invalid when the liquid-phase layer is shallow because of cooler air temperatures. In such cases, upwelling radiation from the ML depends on both surface radiation and cloud water below the ML. This joint dependence makes the evaluation of scattering in the MPL difficult. It has been suggested by K. Aonashi (2005, personal communication) that nonsaturation effects may become negligible when the ML height exceeds 2 km.

Frequent IR observations by geostationary satellites can describe large-scale rainfall distributions and short-term variations, but they cannot describe internal cloud structures. Rainfall estimates from IR observations improve when IR observations are augmented with microwave scattering information (Adler et al. 1993) and lightning information (Morales and Anagnostou 2003), which detect convective regions within clouds. Despite a long history of IR observations, however, the relationship between lightning occurrence and IR TBB remains elusive.

Climatic studies of lightning frequency based on satellite observations have shown that lightning in the Tropics is more frequent over continents than oceans

(Boccippio et al. 2000; Petersen and Rutledge 2001). This land–ocean difference in lightning frequency has been explored using cloud physical analyses that are integrations of PR, TMI, and LIS observations (Nesbitt et al. 2000; Cecil et al. 2002; Cecil and Zipser 2002). Radar reflectivity above the ML is larger over land because there are more large hydrometeors (hail, large graupel, and large raindrops) in the MPL over land than over the ocean. Despite the strong scattering by the large hydrometeors, the observed PCT is larger over continents than over oceans for systems with the same flash rate, because microwave radiation from abundant supercooled cloud water increases the PCT (Toracinta et al. 2002). The existence of both graupel and supercooled cloud water favors charge separation. As expected, lightning is frequently observed by LIS over continents. Observed radar reflectivity profiles show that large graupel and supercooled water are much less common above the ML in precipitating clouds over the ocean, where lightning is not as active. Recently, Cecil et al. (2005) noted that precipitation systems with similar radar reflectivity profiles and PCTs show more frequent lightning over land than over ocean. They speculated that differences could be related to several cloud physical processes that cannot be determined from TRMM-PR and TMI observations, such as a higher cloud base over land, for example.

Our current knowledge of large-scale lightning frequency at midlatitudes is poor. Winter thunderstorms occur frequently along the west coast of Japan as convective clouds form in the unstable layer that develops as flow in the winter monsoon is heated from below over the Sea of Japan. Takeuchi et al. (1978) and Brook et al. (1982) noted that electrical fields are similar in the winter and summer thunderstorms. Electrical fields in both are characterized by a dipole structure, with positive charge aloft. However, the vertical extent in winter is shallower. Takahashi (1984) used results from a numerical simulation of a wintertime thunderstorm to show that riming electrification is important. A major part of the Sea of Japan is beyond the coverage of TRMM observations. Winter thunderstorms, however, are widespread over midlatitude oceans (Kawasaki and Yoshihashi 1999). A part of these thunderstorms can be observed by TRMM.

Cecil and Zipser (2002) used TRMM multisensor observations of PR, TMI, and LIS to investigate the microphysical properties of tropical precipitation systems. TRMM observations are used in this study to examine the microphysical properties of precipitating clouds during winter over midlatitude oceans, with a focus over the western North Pacific, and results from Cecil and Zipser over the tropical ocean are compared to midlatitude results from this study. Cecil et al. (2005) studied three years of lightning frequency in the Tropics and the subtropics and its relationship to the physical properties of clouds in precipitation systems. They confirmed the results of Cecil and Zipser (2002) and detailed land–ocean differences. Computer limitations preclude an investigation that examined for sample size as large as that reported by Cecil et al. (2005). The main conclusions in this paper are based on TRMM data statistics from two months. This study uses 4385 precipitation system samples versus the 5 726 990 of Cecil et al. (2005). Results are, however, representative of the midlatitude precipitation systems over the western North Pacific in winter. This is because lightning frequency during the study period was close to the 6-yr average over the study area.

The first half of this study describes seasonal variations in lightning frequency and its relation to precipitation over midlatitude oceans. Synoptic analyses reveal the relation between winter lightning and extratropical cyclones and cold winter monsoon outbreaks. The second half of the paper uses TRMM observations from PR, TMI, VIRS, and LIS to reveal microphysical properties of precipitating clouds over the western North Pacific in winter. The analyses follow the methods proposed in Cecil and Zipser (2002) but are modified to incorporate analyses of VIRS infrared observations. The results of this study are compared to the results from the Tropics reported in Cecil and Zipser (2002).

2. Data and analysis procedures

Monthly near-surface rain and flash rates for 6 yr between 1998 and 2003 have been analyzed using the PR heating (PRH) grid data (Kodama et al. 2005), which is a climatic dataset including 2.5° gridded statistics of precipitation and flash rate observed by TRMM-PR and TRMM-LIS. Statistics of near-surface rain and flash rate were derived from the version 5 2A25 product provided by the National Aeronautics and Space Administration (NASA) Goddard Space Flight Center (GSFC) and the version 4.1 LIS science data provided by the NASA Marshall Space Flight Center, respectively. Near-surface rain is defined in the PR observations as precipitation at the lowest level that is free of surface clutter. This usually includes precipitation at several levels between 0 and ~2 km (NASA GSFC 2001). The flash rate is defined in this study as the flash counts per unit area normalized by the LIS view time. A flash is defined as a group of continuous and contiguous lightning events within 330 ms in time and 5.5 km in space. An event occurs when LIS observes ra-

TABLE 1. The flash rate (10^{-3} counts per square kilometer per day) averaged over the study area (25°–36°N, 140°–150°E).

Yr	1998	1999	2000	2001	2002	2003	Mean
Jan	1.15	1.50	3.80	1.92	5.70	3.58	
Feb	1.58	0.61	1.48	0.42	2.27	1.01	
Two-month mean	1.35	1.08	2.70	1.21	4.07	2.36	2.12

diation at 777.655 nm, exceeding a threshold. The threshold reduces the influence of background noise. LIS sampling is constrained by a low-view-time limit (~80 s) that combined with a preliminary detection efficiency estimate of 75% yields an effective minimum rate of about one flash per minute (Boccippio et al. 2000). Cumulative LIS view time peaks near 35°N and 35°S (i.e., the northern and southern boundaries of the TRMM orbits, which are the latitudes of the most frequent TRMM observations). The flash rate is defined as flash counts normalized by LIS view time. The flash rate describes lightning frequency free from view-time differences.

Cloud structures and the microphysics of winter thunderstorms are considered in the second part of this study using flash counts obtained from LIS observations and various TRMM data products obtained from PR, TMI, and VIRS observations. There is an overwhelming amount of native resolution TRMM data. Data are reduced to manageable sizes by confining the study area for analyzing cloud microphysics to the area east of Japan over the western North Pacific (25°–36°N, 140°–160°E) and the time period to January and February 2000. Table 1 shows interannual variations in the flash rate in January and February averaged over the study area derived from the PRH grid data. The flash rate in January 2000 was ~1.8 times larger than the six-season mean. The flash rate during the entire study period (i.e., January and February 2000) was about 1.3 times larger than the six-season mean because the flash rate in February 2000 was less than the average. Statistics in January and February 2000 include lightning conditions both higher and lower than the mean values. Version 6 TRMM data products of PR (2A25), TMI (1B11), VIRS (1B01), and version 4.1 LIS science data were used for the microphysical analysis. NASA GSFC (2001) provides details on the data preparation algorithms.

Horizontal resolution differs for each instrument and is 4.3 km for PR, 2 km for IR, approximately 9–16 km for TBB at 37 GHz, approximately 5–7 km for TBB at 85 GHz, and 4 km for LIS. All data were therefore resampled for intercomparison to a 0.05° (latitude) × 0.05° (longitude) grid. Except for flash counts, resampled gridpoint values in the new coordinates were the value at the closest point in the original coordinates. There was no interpolation. Resampled gridpoint values of flash counts were defined as the number of flashes within a 0.05° square centered on the grid point. Differences in observation swaths among the sensors mandated that the study area be confined to the PR swath, which was narrowest, when sensor data were compared. The 6-hourly reanalysis data from the National Centers for Environmental Prediction–National Center for Atmospheric Research (NCEP–NCAR) describe the synoptic situation and define air temperature profiles used to evaluate the heights of cloud tops, ML, MPL, and other variables.

3. Seasonal variation in lightning over midlatitude oceans

Figure 1 shows 6-yr averages of the flash rate and near-surface rainfall for each season. In midlatitudes north of 25°N, heavy precipitation and frequent lightning occurred over western portions of the ocean in summer, but stretched zonally over the entire midlatitude ocean in winter. This is consistent with findings by Petty (1995), who noted that ships more frequently report lightning and strong convective rain in winter over midlatitude oceans. Heavy precipitation reflects the low-latitude portion of the large-scale precipitation zones over midlatitude oceans that developed near storm tracks (Xie and Arkin 1997; Janowiak et al. 1998; Kodama and Tamaoki 2002). Kodama and Tamaoki (2002) pointed out that seasonal extensions of heavy precipitation over the ocean in fall and winter occur not only because of shifts in storm tracks to lower latitudes but also by the extension of heavy precipitation to latitudes south of the tracks. In fall and winter, the precipitation zones arise as deep precipitating clouds develop around fronts and near cyclones, and as shallow precipitating clouds develop behind and to the south of cyclones as cold postfrontal air is warmed and moistened by the relatively warm underlying ocean (Kodama and Tamaoki 2002).

4. Synoptic situation supporting lightning over the western North Pacific during winter

Figure 2 shows day-to-day flash variations superimposed on 925-hPa streamlines and air temperatures

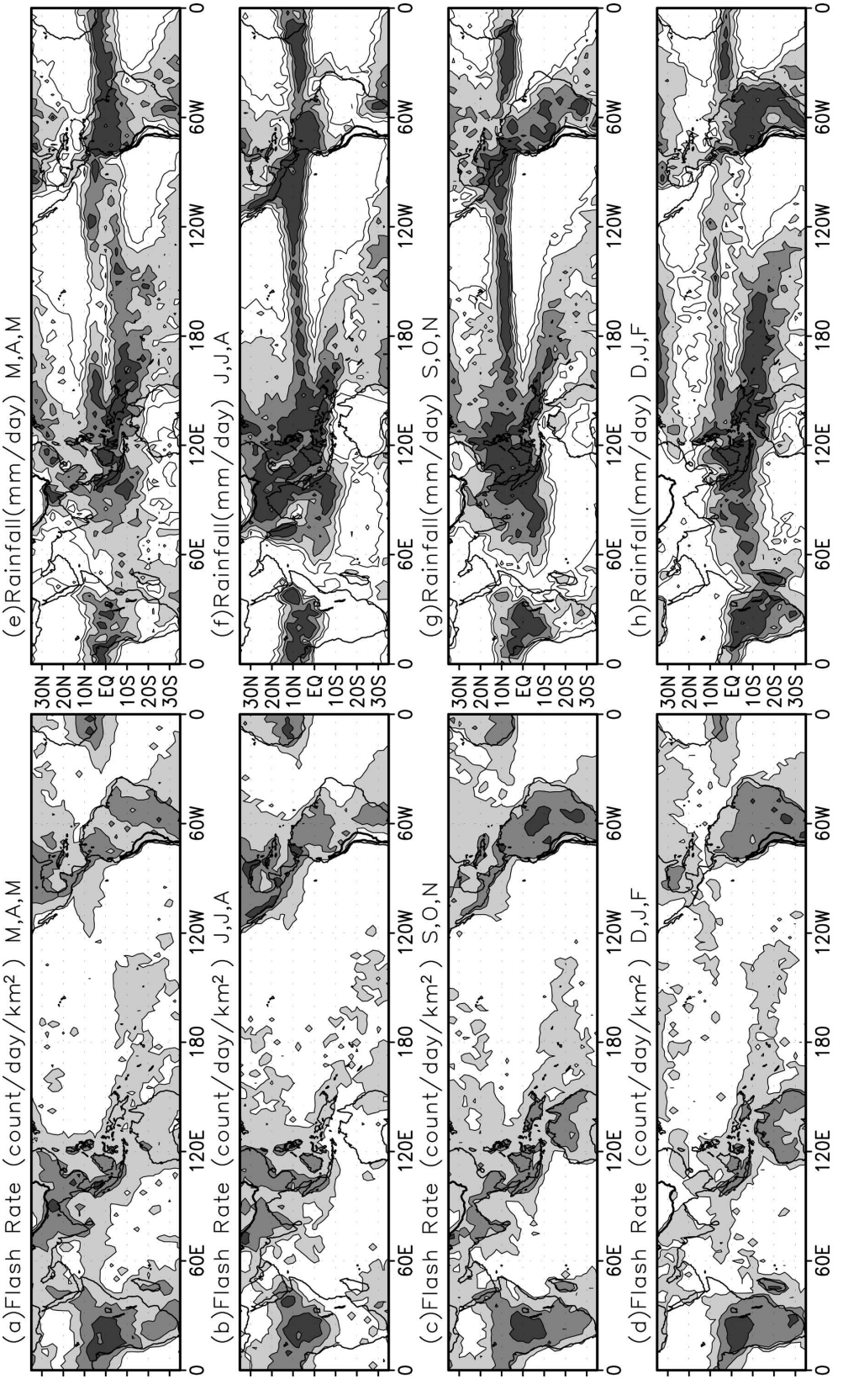

FIG. 1. (a)–(d) Seasonal flash rate observed by TRMM-LIS averaged for 6 yr between 1998 and 2003. (e)–(h) Same as in (a)–(d), but for the intensity of the near-surface rainfall observed by TRMM-PR.

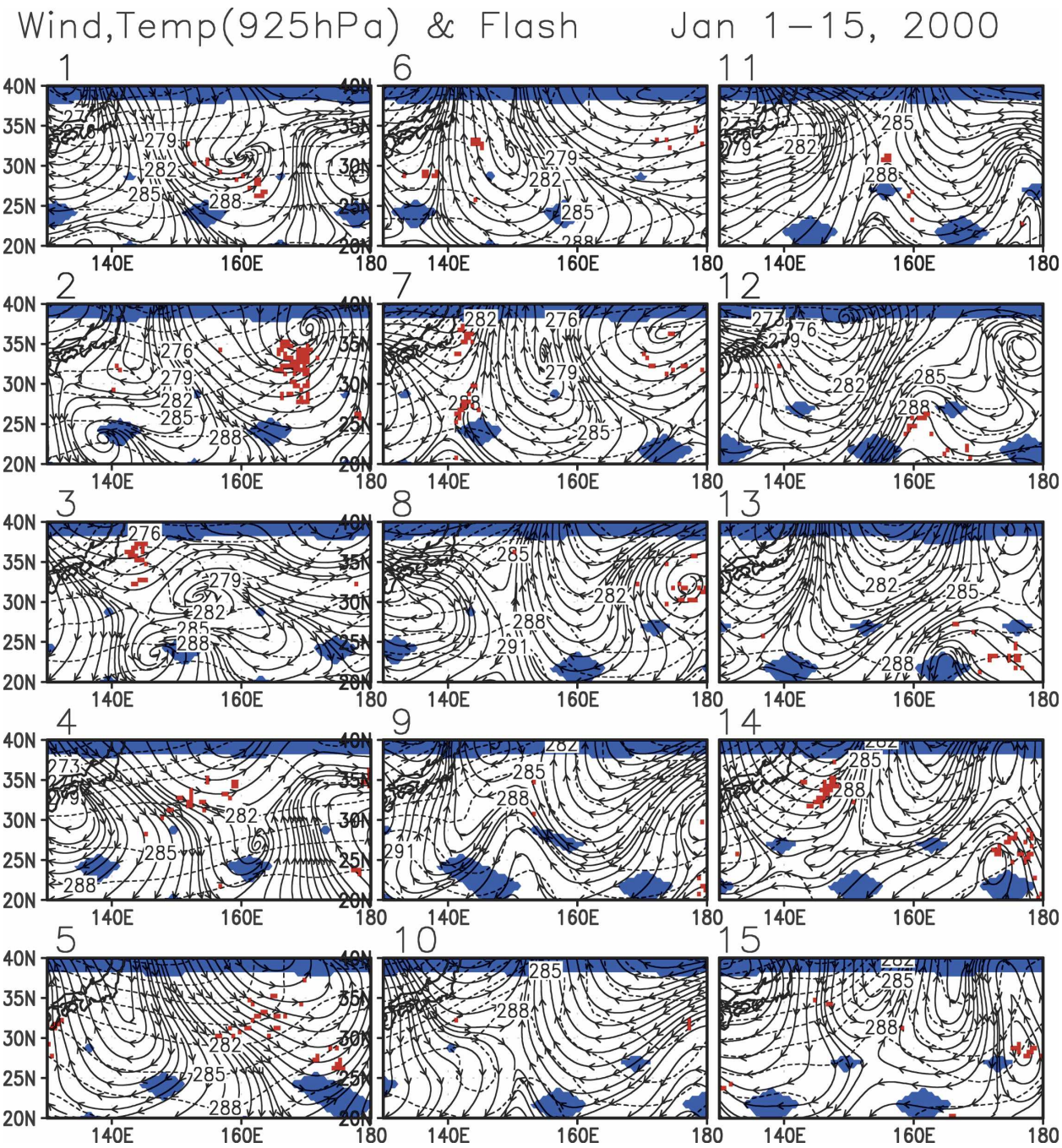

FIG. 2. Day-to-day variations of wind (streamlines) and temperature (dashed contours) at 925 hPa and flash positions (small red squares) during the first half of January 2000. Blue shading indicates the areas with no LIS views.

over the western North Pacific during the first half of January 2000. Wind and temperatures used in Fig. 2 originated from the NCEP–NCAR reanalysis. Despite poor sampling times (approximately 0–350 s day^{-1}) in the LIS observations, the relationship between lightning frequency and synoptic situation is clear. Flashes were near cyclones and/or fronts, such as cyclone centers on 2, 8, 12, 13, and 14 January, and fronts on 4, 6, 7, 11, and 14 January, which can be suggested by strong cyclonic curvature and/or convergence of winds. Some flashes were also observed in cold-air outbreaks behind cyclones on 5, 6, and 15 January. Strong northwesterly winds, cold advection, and diffluent winds characterize these cold-air outbreaks. A similar relationship be-

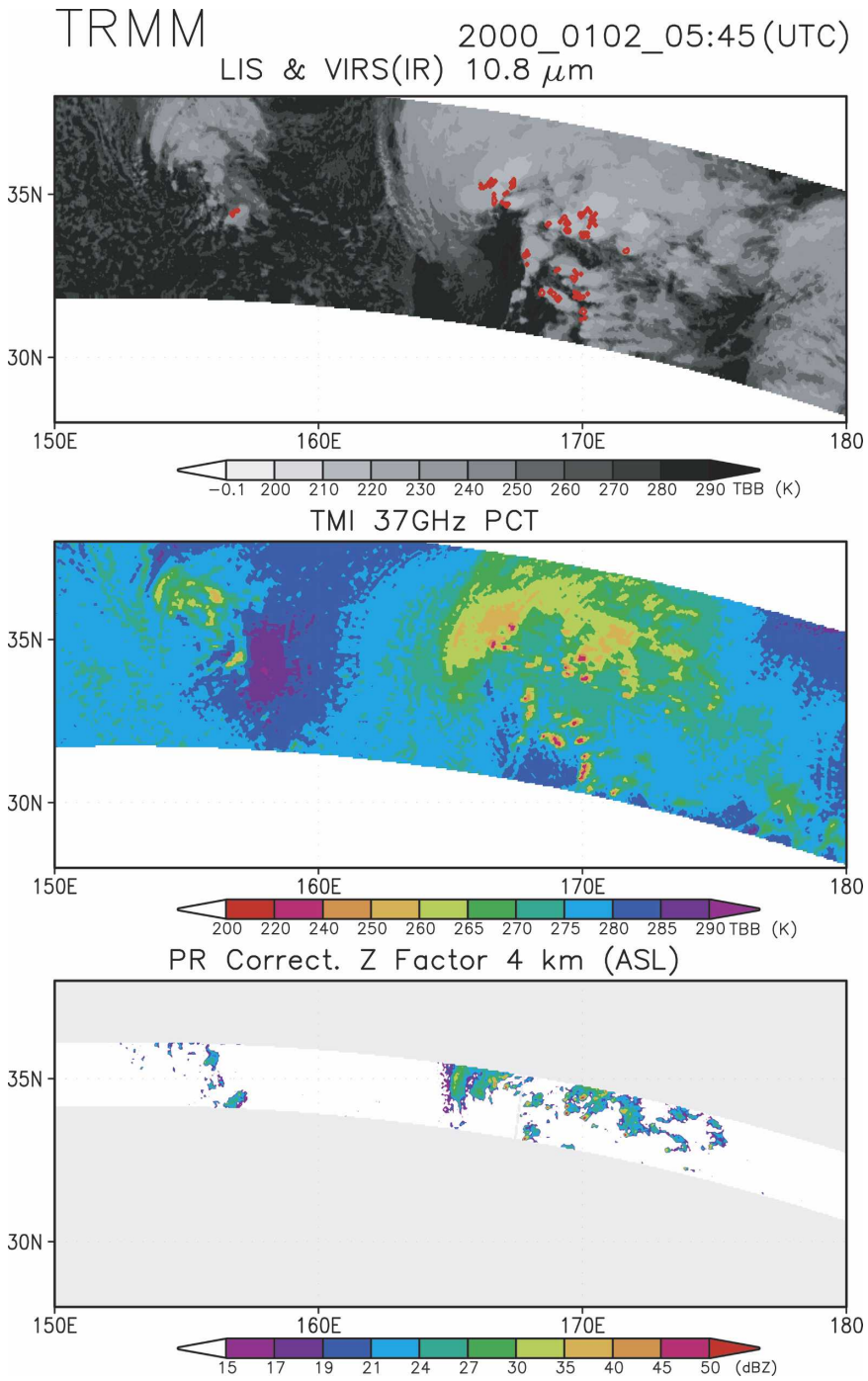

FIG. 3. (top) Flashes (red dots) observed by LIS and TBB at 10.8 μm observed by VIRS around developing cyclones over the western North Pacific. (middle) Same as in the (top), but for PCT37 derived from TMI observations. (bottom) Same as in the (top), but for the corrected Z factor at 4 km MSL from PR observations. The observation swath is narrower for the PR.

tween the flashes and synoptic situation occurred in 2000 during the rest of January and in February.

Figure 3 shows flashes superimposed on a field of 10.8-μm TBB (top panel), of PCT37 (middle panel), and of the attenuation-corrected Z factor at 4 km MSL (bottom panel), for an example with frequent flashes near a cyclone center near 170°E. The 4-km height was selected because 4 km MSL corresponded to about

−12°C in the NCEP–NCAR reanalysis data, although spatial and temporal variations in air temperature were large around the cyclone center. Thus, radar reflectivity in the MPL of the clouds could be examined. Cecil and Zipser (2002) used 7 km MSL, corresponding to approximately −10° to −15°C in the Tropics, as a reference level for the reflectivity in the MPL of clouds. The −12°C level is used as a reference level in the MPL in the present study. Most flashes occurred in small regions where reflectivity exceeded 40 dBZ and PCT37 was cooler than 260 K. Regions of low PCT37 and large reflectivity in the MPL indicate the existence of large graupel that is sustained by active deep convection (Cecil and Zipser 2002; Toracinta et al. 1996). The statistical relationship among lightning frequency, radar reflectivity at −12°C, and PCT37 is examined later. Reflectivity cores were commonly accompanied by cloud streaks that extended to the east. These were likely anvils in the upper troposphere extending into the prevailing westerly winds from deep convective clouds.

Figure 4 shows several flashes that appeared in scattered shallow clouds that developed in a cold-air outbreak west of a cold front near 170°E. Flashes were observed in clouds where PCT37 was at a local minimum. The horizontal extents of these scattered clouds were comparable to the footprint in the 37-GHz channel (approximately 9–16 km), so nonuniform beamfilling effects may have affected the minimum PCT37. Errors in capturing flashes may have also arisen because of the short LIS view time for each cloud. Statistical results discussed below suggest a relationship among minimum PCT37, radar reflectivity, and cloud-top height.

5. Microphysical characteristics of precipitation features

A statistical analysis of 300 scenes of TRMM observations over the western North Pacific (approximately 25°–36°N, 140°–160°E) during January and February 2000 clarified microphysical properties of precipitating clouds and their relationship to lightning frequency over oceans in winter. Data processing followed Cecil et al. (2002) with several modifications. First, precipitating systems had to consist of at least three contiguous 0.05° grid squares (~75 km^2) in which attenuation-corrected near-surface radar reflectivity exceeded 20 dBZ. These thresholds were similar to those in Cecil et al. (2002). However, a threshold was not used for PCT85, because PCT85 may be influenced by large variations in air temperature and ML height (e.g., Grody 1991), which are common during midlatitude winter. Selected precipitation systems are referred to as "precipitation features" following Cecil et al. (2002). Flashes were counted for each feature, and each feature included precipitating clouds in various stages of development. Second, additional analyses were performed using minimum TBB and maximum cloud-top height derived from IR observations from VIRS.

Cecil and Zipser (2002) investigated minimum PCT and maximum radar reflectivity for each feature in the Tropics to examine the most intense convection observed by each sensor. These most intense values tend to occur in about the same location. Their approach was adopted in this study; maximum radar reflectivity, minimum PCT85 and PCT37, and minimum TBB at 10.8 μm (equivalently, maximum cloud-top height) were compared to the number of flashes.

Toracinta et al. (1996) and Cecil and Zipser (2002) showed that active flashes are likely where large radar reflectivity and small lapse rates in MPL reflectivity overlap. Lightning is likely where large graupel, hail, and large supercooled raindrops exist in abundance in the MPL, resulting in a small vertical reflectivity lapse rate and indicating vigorous convection with vigorous updrafts that can suspend large hydrometeors far above the ML. Cecil and Zipser (2002) referenced a maximum reflectivity at 7 km MSL and a lapse rate of reflectivity between 6 and 9 km in the MPL in their examination of precipitating clouds in the Tropics. The reference heights 6, 7, and 9 km correspond to air temperatures of −6°, −12°, and −24°C, respectively, in the Tropics as determined from the NCEP–NCAR reanalysis (not shown). Air temperature profiles, which greatly influence cloud microphysics, showed large spatial and temporal variations in the present study area. The vertical structure of the precipitation feature was therefore described by air temperature profiles or relative height above the ML. The height of reference levels was determined from current air temperature profiles obtained by time interpolating the 6-hourly NCEP–NCAR reanalysis data for each feature at the 0°, −6°, −12°, and −18°C levels. The ML was defined as the 0°C level. Reflectivity lapse rates were computed between the levels at −6° and −18°C. A reference temperature of −18°C was used instead of −24°C because most precipitation features in the study area were shallower than those in the Tropics. Echo tops in the study area were rarely colder than −24°C.

Figure 5 shows the cumulative density of maximum radar reflectivity as a function of height above the ML at several different percentiles. The 99th percentile profiles for tropical precipitation features above the ML averaged over continents and oceans, from Cecil et al. (2002), are shown for comparison. The ML in the Tropics was assumed to be at 4.75 km based on a mean

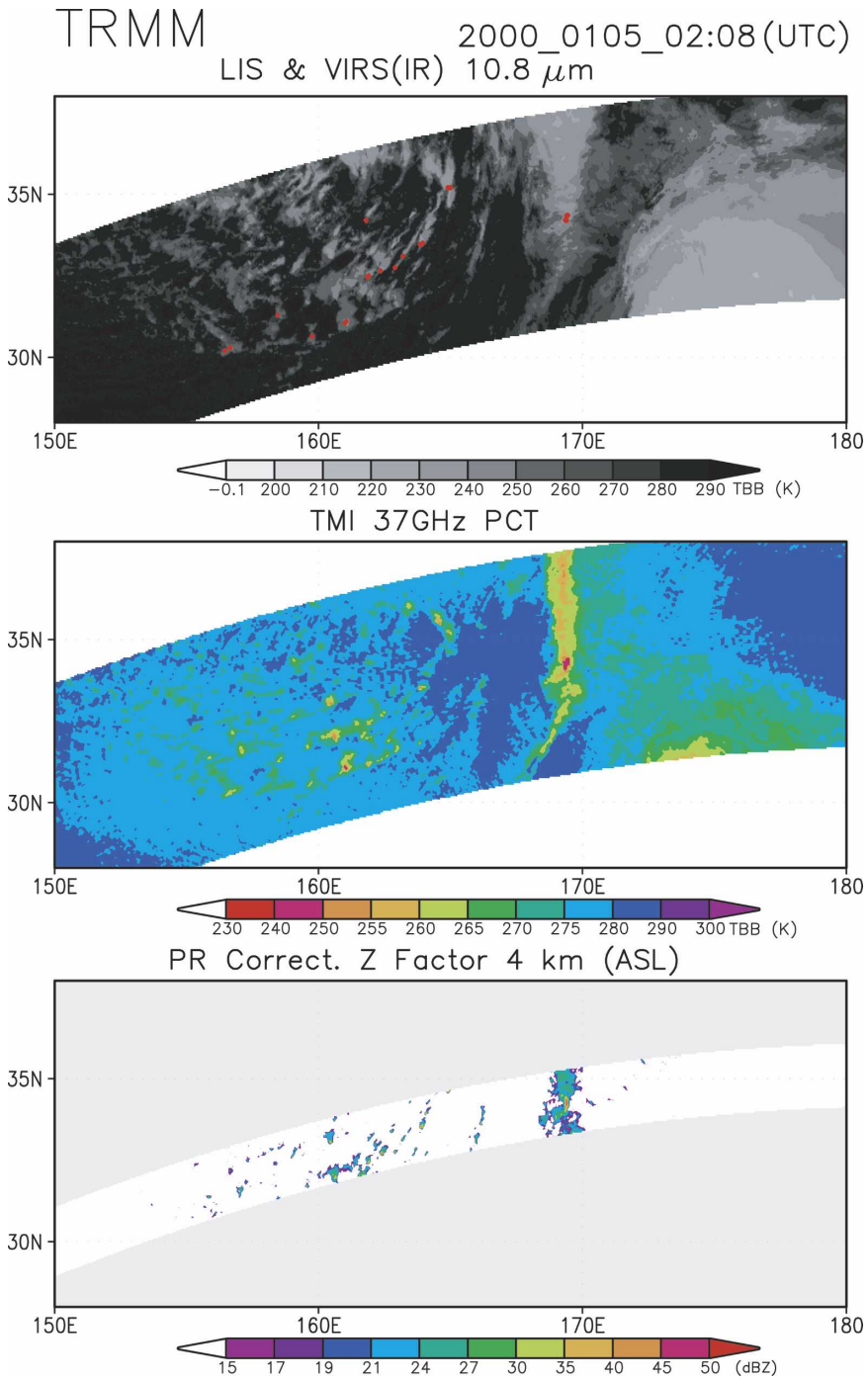

FIG. 4. Same as in Fig. 3, but around and behind a cold front (~170°E), where cold air was warmed and moistened by the underlying ocean.

temperature profile derived from the reanalysis. Cecil et al. (2002) noted that the lapse rate of radar reflectivity above the ML in the Tropics is much smaller over continents than over oceans. This means that tropical convection is stronger over continents. In the layer approximately 2–4 km above the ML, the 99th percentile profile for the tropical oceans was located between the 99th and 99.9th percentile profiles for the winter ocean and was parallel to those profiles. In the layer higher than 4 km above the ML, the lapse rate was much larger for the winter ocean cases. A similar lapse rate below 4 km suggests that active convective features comparable

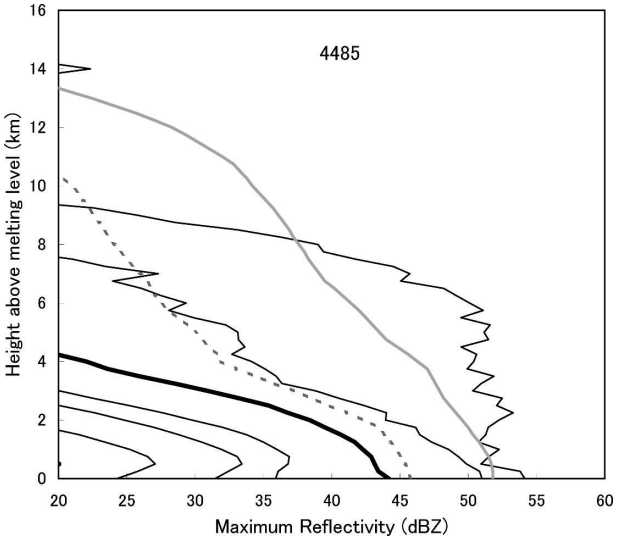

FIG. 5. Vertical profiles of the cumulative density function of the maximum reflectivity of the precipitation features above the melting level. (left to right) Profiles at the 75th, 90th, 95th, 99th (thick), 99.9th, and 99.99th percentiles. The sample size is listed. The ordinate represents the height relative to the melting level. The profiles of the 99th percentile for the tropical ocean (gray dashed line) and tropical continents (gray line) from Cecil et al. (2002) are shown for comparison.

to those over the tropical oceans exist over the western North Pacific in winter, although the vertical extent of convection was lower and the relative number of active convective features was smaller in winter.

Minimum PCT37 and minimum TBB at 10.8 μm are compared in the left panel of Fig. 6. Gray (black) circles indicate systems without (with) flashes. The size of the black circle denotes the number of flashes observed over each precipitation feature. Lightning frequency depended strongly on minimum PCT37, as noted by Cecil and Zipser (2002) for the Tropics, and depended weakly on the minimum TBB. The relationship between the minimum PCT37 and the maximum cloud-top height (right panel) was examined because the TBB is affected by variations in both air temperature and cloud top. The approximate cloud-top height was determined by assuming that TBB at 10.8 μm, the cloud-top temperature, and the air temperature at the cloud-top level were the same. Air temperature profiles were obtained by time interpolating the 6-hourly reanalysis data. When features were characterized by a maximum cloud-top height above 10 km, flashes accompanied most features characterized by a minimum PCT37 less than 255 K. Shallower features with cloud tops below 10 km were characterized as flash and nonflash regions divided by a transitional zone of 250–270 K. No significant criteria were found in cloud-top height for these features; flash and no-flash features coexisted between 5 and 16 km. Lightning frequency was more sensitive to PCT37 than to cloud-top height, indicating that lightning was more sensitive to the existence of large hydrometers in the MPL of clouds.

Figure 7 compares minimum PCT85 and maximum cloud-top height. The percentage of features with lightning gradually increased as the minimum PCT85 decreased between 150 and 250 K. Changes in minimum

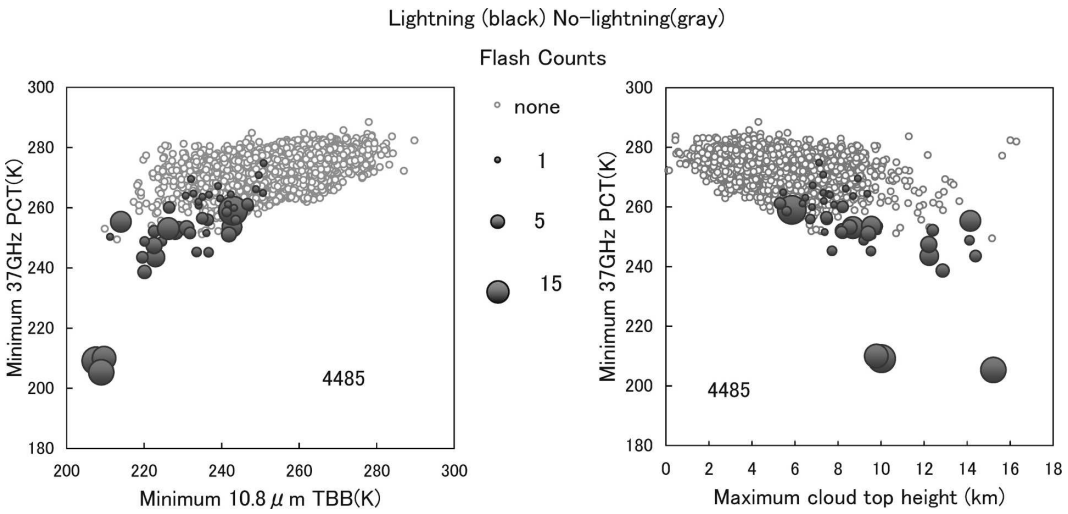

FIG. 6. (left) Minimum PCT37 vs minimum TBB at 10.8 μm for precipitation features. Black (gray) circles correspond to features with (without) lightning. The size of the black circles reflects the number of flashes within each feature. Sample size is listed. (right) Same as in (left), but for the maximum cloud-top height instead of minimum PCT37. The cloud-top height was derived from the minimum TBB at 10.8 μm.

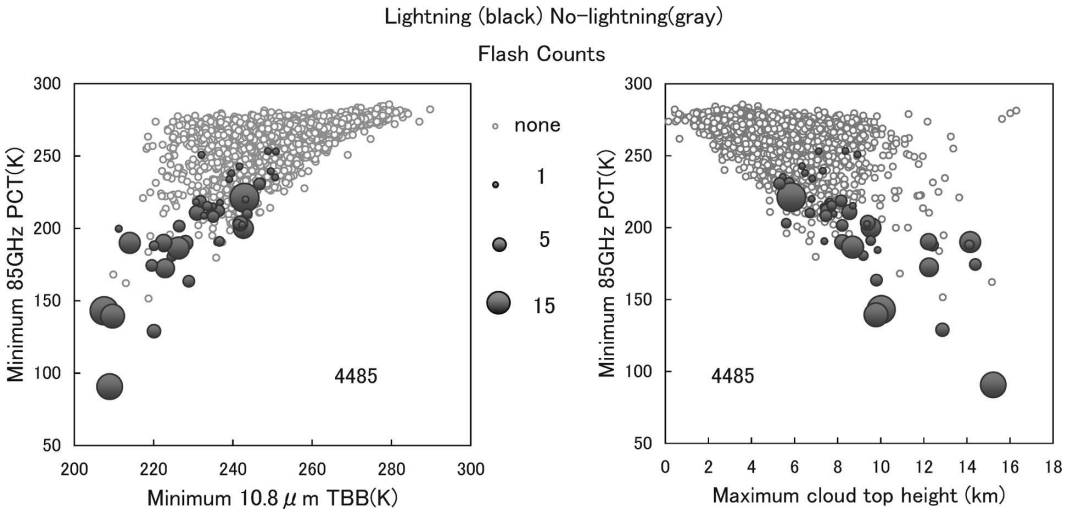

FIG. 7. Same as in Fig. 6, but for minimum PCT85 instead of minimum PCT37.

PCT85 had a smaller effect on lightning than changes in minimum PCT37 because lightning frequency is more sensitive to the existence of large hydrometeors, which impact PCT37 measurements, than to the existence of upper-level ice particles, which impact PCT85 measurements. For shallower features with tops below 10 km, however, the division between lightning and no-lightning systems was weaker for both PCT37 and PCT85. Reasons for the difference remain elusive. The weaker division in PCT37 for the shallower features may be related to nonuniform beamfilling effects and unsaturated upward emission at the top of thin liquid-phase layer.

To evaluate the above hypothesis, Fig. 8 compares minimum PCT37 and maximum cloud-top height for features classified under two different conditions. The left panel compares when the ML height was higher than 2 km. Two-thirds of the features in the present study were excluded when the ML height was restricted to be higher than 2 km. Most of the excluded cases occurred when cold-air outbreaks occurred over the ocean (not shown). Shallow flashed features with a maximum cloud top lower than 6 km MSL disappeared. The excluded cases occurred in the cold-air outbreak, when the ML layer height decreased. The right panel compares when small features were excluded. Here the

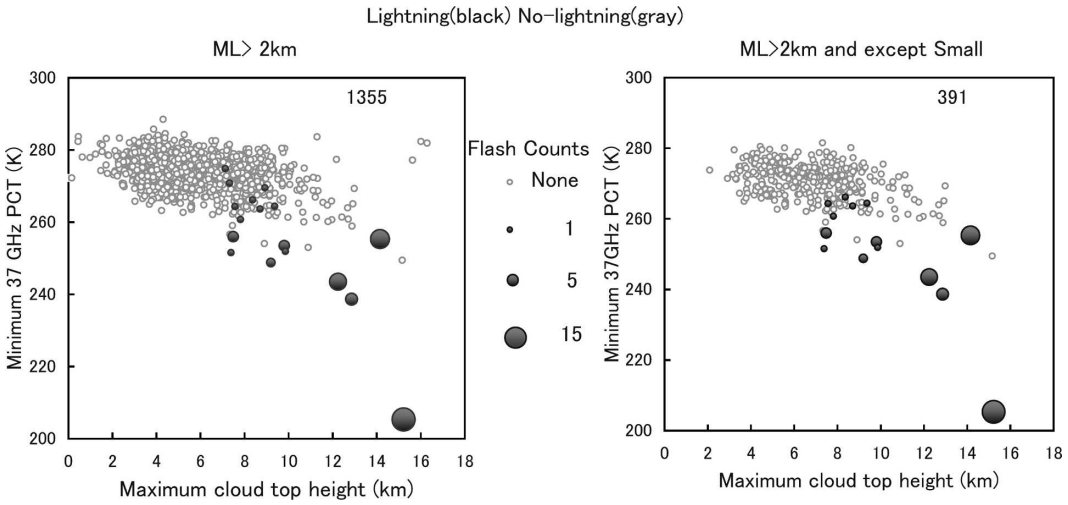

FIG. 8. (left) Same as in the right panel of Fig. 6, but for the features when melting level is higher than 2 km MSL. The sample size is listed. (right) Same as in (left), but the melting level is higher than 2 km MSL and the size of the features is more than 10 grids.

small features are defined to have 10 or less contiguous grids. An area of 10 grids corresponds to 750 km^2. Considering the footprint size of the 37-GHz channel of TMI is ~120 km^2, partial beamfilling is likely to occur frequently for these small features. Flashed features with the highest three values of PCT37 were removed in the panel. This suggests that PCT37 in these features may not represent the true value in precipitation clouds due to partial beamfilling by small clouds. However classification by cloud size is an incomplete method to detect the features influenced by partial beamfilling. After applying these conditions, the division of flashed and nonflashed features was improved. We also applied these two conditionings for PCT85. Shallow flashed features were removed as in Fig. 8 but flashed features of higher PCT85 were kept (not shown). The division of flashed and nonflashed features was not improved as in PCT37.

Results in Figs. 6, 7, and 8 are summarized as follows. Most flashes occur in features characterized by a minimum PCT37 colder than around 260 K. The minimum PCT37 criterion was more accurate and close to 255 K for features with cloud tops above 10 km. Large hydrometeors in the MPL support the presence of lightning (Cecil and Zipser 2002). High cloud tops alone cannot be used to predict lightning. PCT37 can be used to classify lightning and nonlightning features, although nonuniform beamfilling effects due to a large footprint at 37 GHz and unsaturated upward radiation due to the shallow liquid-phase layer may influence PCT37.

Toracinta et al. (2002) and Cecil and Zipser (2002) related the probability of lightning in tropical precipitation features to the minima in PCT37 and PCT85. They noted that for each minimum PCT, probabilities were larger for features over continents than over the ocean. The difference arise from upward emissions from supercooled cloud water in the MPL; such emissions may be greater in features over continents than over oceans, and this effect may be more prominent for the minimum PCT85 than the PCT37 (Adler et al. 1991). Figure 9 compares the relationship in the present study to results by Cecil and Zipser (2002). The features with the ML height lower than 2 km were excluded before calculating the relationship, because the thin liquid-phase layer may influence PCTs as discussed before. For the same probability of lightning, both PCTs lay between corresponding values over the tropical oceans and continents. This may suggest that precipitation features with lightning in the present study contained supercooled cloud water, even though the moisture content in the lower troposphere was smaller because of lower air temperature than in the Tropics. However, the vertical structure of precipitation features may have affected the differences in PCT85 and PCT37. Because the vertical extent of vigorous convection above the ML was smaller in precipitation features in the present study (Fig. 5), supercooled cloud water was warmer and may have more efficiently radiated microwaves in those features with lightning than in similar features in the Tropics. Comparisons of the amount of supercooled water in features in the present study and in the Tropics will require further study using a radiative transfer model to examine the influence of the vertical distribution of supercooled water in precipitation features and the influence of ML height variation. Hereafter, we show the results without conditioning the features by their size or environmental ML height, because these conditionings largely diminish the numbers of samples.

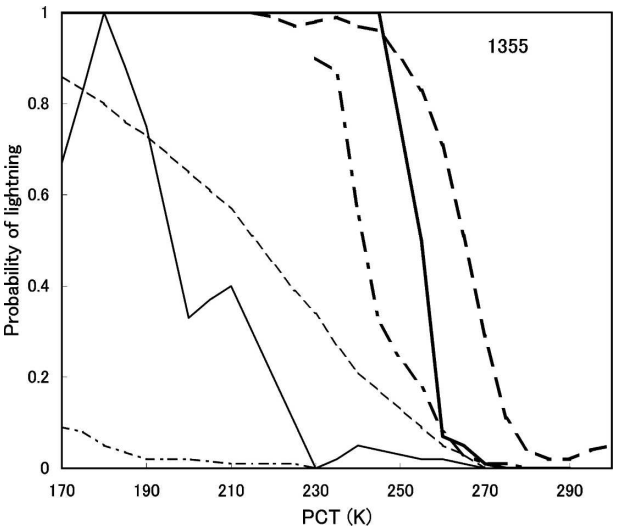

FIG. 9. Probability of lightning in precipitation features as functions of the minimum PCT37 (thick solid line) and the minimum PCT85 (thin solid line) for the features when melting level was higher than 2 km. Corresponding dashed (dash–dotted) lines are for precipitation features over tropical continents (oceans) from Cecil and Zipser (2002). The sample size is listed.

Toracinta et al. (1996) and Cecil and Zipser (2002) described a relationship between lightning and strong radar reflectivity cores with a slower decrease in reflectivity with height in the MPL, suggesting the existence of large graupel and strong updrafts. A similar relationship was found here. Figure 10 compares the minimum PCT37 and the maximum reflectivity at −12°C, a reference level corresponding to the MPL. Flash frequency gradually increased as reflectivity increased from 30 to 40 dBZ, a result similar to findings in the Tropics (Fig. 13 of Cecil and Zipser 2002). Figure 11 shows the dependence of lightning frequency on the lapse rate of maximum reflectivity between −6° and −18°C, and the maximum reflectivity at −12°C, located

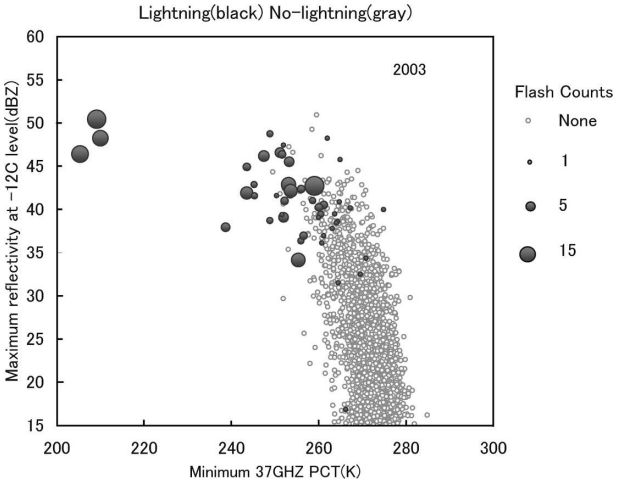

FIG. 10. Maximum reflectivity at the −12°C level vs the minimum PCT37 for the precipitation features. The sample size is listed.

in the MPL. We excluded shallow features in which the reflectivity at −18°C was undetectable. No flashes were observed for such shallow features. Lightning was likely when the lapse rate was small and the maximum reflectivity was large, despite the existence of many no-flash features. When comparisons were made at similar air temperatures, the relationship between radar reflectivity profiles and lightning frequency in the present study area resembled the relationship in the Tropics (Fig. 5 of Cecil and Zipser 2002), despite the smaller vertical extent of features. Previous studies have also shown that lightning frequency is sensitive to air temperature conditions in clouds (Takahashi 1978, 1984).

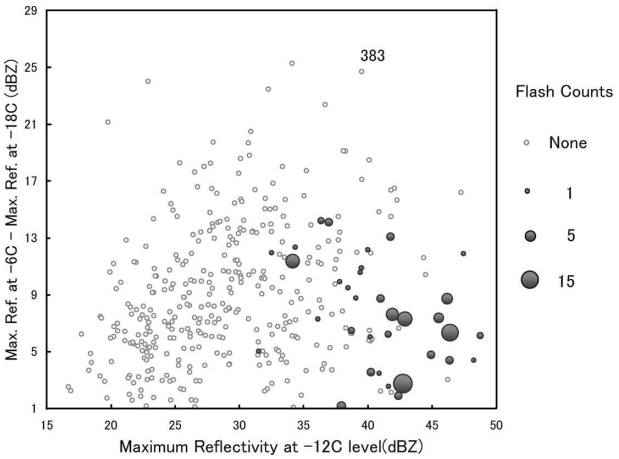

FIG. 11. Maximum reflectivity at −12°C vs the lapse rate of maximum reflectivity between −6° and −18°C. Only the features in which the reflectivity was detectable at both −6° and −18°C are shown. Gray open circles correspond to features with no lightning. Thick open circles correspond to lightning features, and their size represents the number of flashes within each feature. The sample size is listed.

TABLE 2. Number of precipitation features and flashes in the large-scale ascending and descending categories determined from the data for January and February 2000.

Category	Ascending at 600 hPa	Descending at 600 hPa
No. of precipitation features	1343	3142
Tot No. of grids in the precipitation features	5.92×10^4	4.10×10^4
Near-surface rainfall (mm h^{-1}) averaged for the precipitation feature grids	3.36	2.51
No. of flashes	109	76
No. of precipitation features with flashes	29	18
No. of flashes per grid in precipitation features	1.84×10^{-3}	1.85×10^{-3}

6. Comparison between features in conditions of large-scale ascent or descent

Precipitation features can be divided into two categories over the northwestern Pacific during winter. The first category includes precipitation that develops near the centers of cyclones and along their fronts. The second category includes postfrontal precipitation that develops behind cyclones in an environment of strong warming and moistening of cold air over the warmer ocean (cf. Figs. 3 and 4). The physical mechanisms that support the precipitation differ greatly between the two categories. Features are classified into "ascending" and "descending" environments according to large-scale omega at 600 hPa in the NCEP–NCAR reanalysis data. This classification by omega allows an examination of the dependence of microphysical properties on the categorization, because large-scale midtropospheric ascent (descent) dominates in the first (second) category.

Table 2 shows statistics for near-surface rainfall and lightning frequency in precipitation features for the two categories. The number of precipitation features was much larger for descending conditions, but the total number of precipitation feature grids was smaller in the descending conditions. This means that the mean horizontal extent of precipitation features was much larger for ascending conditions. The near-surface rainfall averaged for grids in precipitation features was larger in the ascending condition. Thus, precipitation features in the ascending category contribute two-thirds of the total rain but the contribution of the descending category was also large, in agreement with conclusions by Kodama and Tamaoki (2002), who commented on a

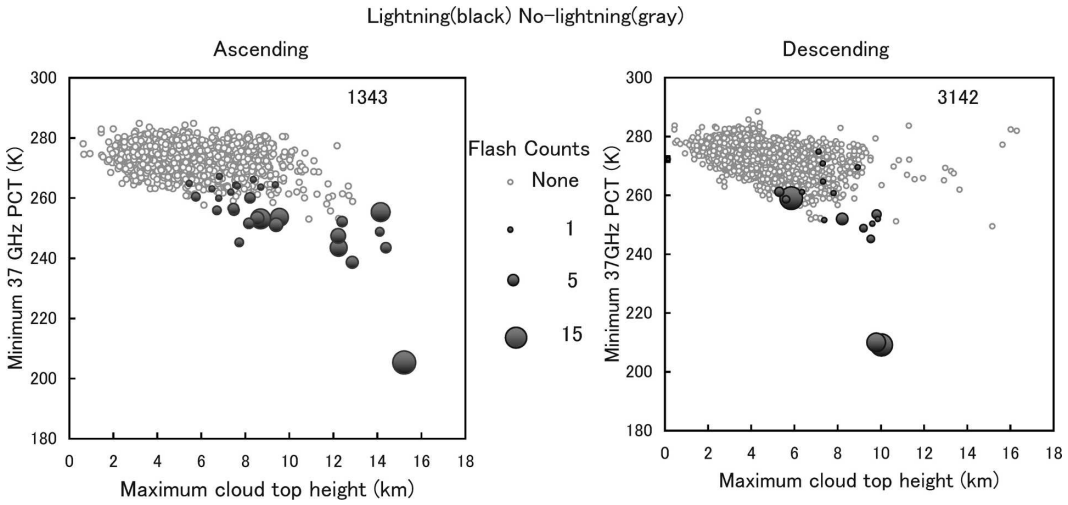

FIG. 12. Same as in the right panel of Fig. 6, but for features in the (left) ascending and (right) descending conditions.

large contribution to precipitation from shallow clouds to the rear of cyclones. The number of flashes per grid in the precipitation features was comparable between the categories.

Figure 12 compares minimum PCT37 and maximum cloud-top height, as in the right panel in Fig. 6, but for each category. Three features with PCT 37 more than 268 K are observed in the descending category. These are small features that were discussed in Fig. 8. These small features appeared in the cold-air outbreak in the descending conditions. Figure 13 compares the minimum PCT37 and PCT85 for each category. There were no significant differences in the distribution of flashed features between the categories. In addition, no significant differences were evident between the categories for the comparisons made in Figs. 10 and 11 (not shown).

Figure 14 shows cumulative densities of maximum radar reflectivity as a function of height above the ML for several different percentiles as in Fig. 5, but for each category. The 99th percentile profile of maximum reflectivity was larger for features in the ascending category. This means that the relative population of features with vigorous convection was larger in the ascending conditions (i.e., around cyclones and fronts). Nevertheless, the 99th percentile profiles in both categories were lower than those over the tropical ocean, except for the lowest layer in the ascending category.

7. Summary and conclusions

Seasonal variations in precipitation and lightning were described over midlatitude oceans, and TRMM multisensor observations were used to examine microphysical properties and their relationships to lightning frequency for precipitation features over the western North Pacific in winter. Analysis methods in general followed those proposed by Cecil et al. (2002) and Cecil and Zipser (2002). However, some modifications were made. For example, IR data were analyzed using VIRS observations, and large variability in air temperature profiles was considered. Results are as follows:

1) Over the midlatitude oceans in winter, heavy precipitation and frequent lightning flashes stretched zonally near storm tracks.
2) Lightning flashes over the western North Pacific in winter occurred in two regions. Flashes occurred

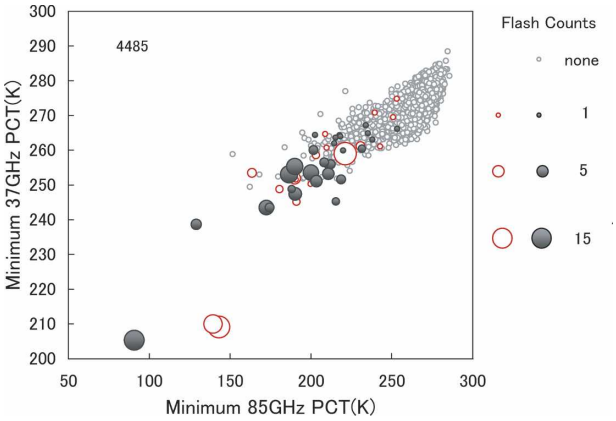

FIG. 13. Minimum PCT85 vs minimum PCT37. Red open (black closed) circles indicate the lightning features in the descending (ascending) conditions. Gray circles correspond to features with no lightning. The sample size is listed.

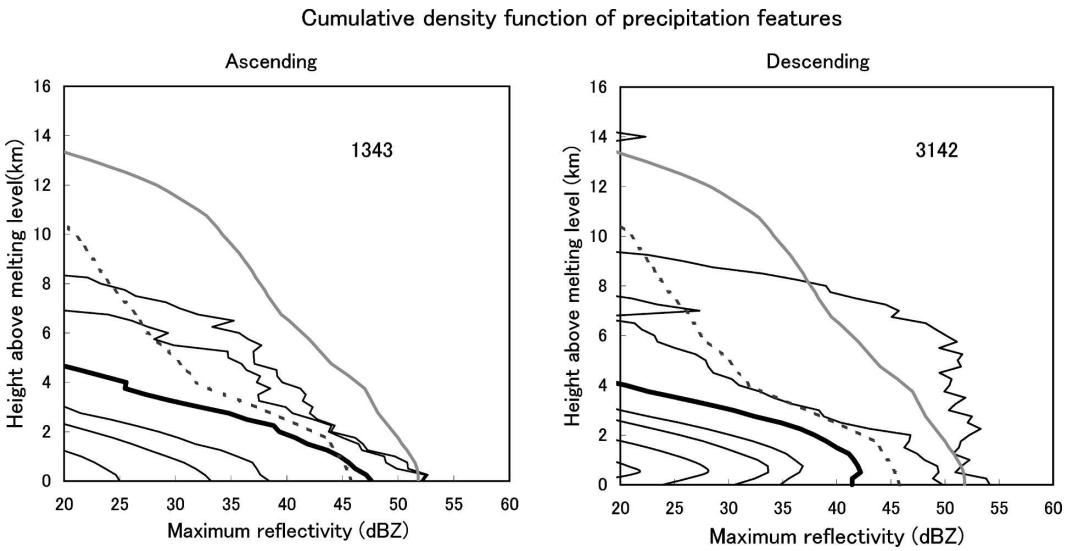

FIG. 14. Same as in Fig. 5, but for precipitation features in the (left) ascending and (right) descending conditions.

near cyclone centers and along fronts. Flashes also occurred in large-scale subsidence behind cyclones, where heating and moistening by the ocean was intense.

3) Lapse rates of maximum radar reflectivity above the ML for precipitation features over the midlatitude ocean in winter were related to convective intensity and comparable to lapse rates over tropical oceans. However, the convective layer characterized by a small lapse rate was much thinner, and the relative number of active convective features was smaller over the midlatitude ocean in winter.
4) Most lightning flashes occurred in features characterized by a minimum PCT37 colder than ~260 K, indicating the existence of large hydrometeors in the MPL. Minimum PCT37 can be used to classify the presence of lightning. Cloud-top and PCT85 data alone provide insufficient information for estimating lightning. The minimum PCT37 criterion was more accurate for features with cloud tops above 10 km.
5) Large radar reflectivity and a small lapse rate within the MPL correlate with lightning frequency as demonstrated by Cecil and Zipser (2002) in the Tropics. The present study included fewer numbers of features with smaller vertical extents, which satisfy these conditions. Nevertheless, relationships between radar reflectivity and lightning frequency were similar to tropical relationships when comparisons were made at the same air temperature.

Greater variability in the structure of precipitating clouds is expected over the midlatitude ocean in winter than over the tropical oceans. The variability also exists between the precipitating clouds that developed near cyclones and the postfrontal clouds behind cyclones during the winter monsoon. Nevertheless, microphysical conditions for lightning over the midlatitude ocean resembled conditions in the Tropics and were consistent with the theory of riming electrification (Takahashi 1978). The influence on observed PCTs by nonuniform beamfilling, unsaturated radiation at the top of the thin liquid-phase layer, and scattering in the Mie regime by large hydrometers is left to be studied. One hypothesis of Cecil et al. (2005) noted that flash occurrence is more frequent over land than over the ocean for similar PCT features and radar reflectivity profiles. They speculated that microphysical processes might accentuate lightning over land. Precipitation over the western North Pacific in winter is influenced by continental air masses. Continental air masses may contain many ice nuclei, so microphysical processes controlling lightning in the midlatitude winter represent an interesting topic for future studies.

Acknowledgments. This study was financially supported as a cooperative study between the Japan Aerospace Extrapolation Agency (JAXA) and Hirosaki University. The authors are grateful to Dr. T. Ushio for flash data processing. Constructive comments by Dr. K. Aonashi and Mr. D. Satoh improved this study. Critical comments from anonymous reviewers were highly useful in improving the manuscript.

REFERENCES

Adler, R. F., H.-Y. M. Yeh, N. Prasad, W. K. Tao, and J. Simpson, 1991: Microwave simulations of a tropical rainfall system with a three-dimensional cloud model. *J. Appl. Meteor.,* **30,** 924–953.

——, A. J. Negri, P. R. Keehn, and I. M. Hakkarinen, 1993: Estimation of monthly rainfall over Japan and surrounding waters from a combination of low-orbit microwave and geosynchronous IR data. *J. Appl. Meteor.,* **32,** 335–356.

Boccippio, D. J., S. J. Goodman, and S. Heckman, 2000: Regional differences in tropical lightning distributions. *J. Appl. Meteor.,* **39,** 2231–2248.

Brook, M., M. Nakano, and P. Krehbiel, 1982: The electrical structure of the Hokuriku Winter Thunderstorms. *J. Geophys. Res.,* **87,** 1207–1215.

Cecil, D. J., and E. J. Zipser, 2002: Reflectivity, ice scattering, and lightning characteristics of hurricane eyewalls and rainbands. Part II: Intercomparison of observations. *Mon. Wea. Rev.,* **130,** 785–801.

——, ——, and S. W. Nesbitt, 2002: Reflectivity, ice scattering, and lightning characteristics of hurricane eyewalls and rainbands. Part I: Quantitative description. *Mon. Wea. Rev.,* **130,** 769–784.

——, S. J. Goodman, D. J. Boccippio, E. J. Zipser, and S. W. Nesbitt, 2005: Three years of TRMM precipitation features. Part I: Radar, radiometric, and lightning characteristics. *Mon. Wea. Rev.,* **133,** 543–566.

Christian, H. J., and Coauthors, 1999: The Lightning Imaging Sensor. *Proc. 11th Int. Conf. on Atmospheric Electricity,* Guntersville, AL, International Commission on Atmospheric Electricity, 746–749.

Grody, N. C., 1991: Classification of snow cover and precipitation using the special sensor microwave imager. *J. Geophys. Res.,* **96,** 7423–7435.

Iguchi, T., T. Kozu, R. Meneghini, J. Awaka, and K. Okamoto, 2000: Rain-profiling algorithm for TRMM precipitation radar. *J. Appl. Meteor.,* **39,** 2038–2052.

Janowiak, J. E., A. Gruber, C. R. Kondragunta, R. E. Livezey, and G. J. Huffman, 1998: A comparison of the NCEP–NCAR reanalysis precipitation and the GPCP rain gauge–satellite combined dataset with observational error considerations. *J. Climate,* **11,** 2960–2979.

Kawasaki, Z.-I., and S. Yoshihashi, 1999: TRMM/LIS observation and lightning activity. *Proc. 11th Int. Conf. on Atmospheric Electricity,* Guntersville, AL, International Commission on Atmospheric Electricity, 176–179.

Kodama, Y.-M., and A. Tamaoki, 2002: A re-examination of precipitation activity in the subtropics and the mid-latitudes based on satellite-derived data. *J. Meteor. Soc. Japan,* **80,** 1261–1278.

——, A. Ota, M. Katsumata, M. Katsumata, S. Mori, S. Satoh, and H. Ueda, 2005: Seasonal transition of predominant precipitation type and lightning activity over tropical monsoon areas derived from TRMM observations. *Geophys. Res. Lett.,* **32,** L14710, doi:10.1029/2005GL022986.

Kummerow, C., W. Barnes, T. Kozu, J. Shiue, and J. Simpson, 1998: The Tropical Rainfall Measuring Mission (TRMM) sensor package. *J. Atmos. Oceanic Technol.,* **15,** 809–817.

——, and Coauthors, 2000: The status of the Tropical Rainfall Measuring Mission (TRMM) after two years in orbit. *J. Appl. Meteor.,* **39,** 1965–1982.

Morales, C. A., and E. N. Anagnostou, 2003: Extending the capabilities of high-frequency rainfall estimation from geostationary-based satellite infrared via a network of long-range lightning observations. *J. Hydrometeor.,* **4,** 141–159.

NASA GSFC, 2001: Tropical Rainfall Measuring Mission science data and information system. Interface control specification between the Tropical Rainfall Measuring Mission science data and information system (TSDIS) and the TSDIS Science User (TSU) TSDIS-P907, Vol. 4: File specifications for TRMM products—level 2 and level 3, 69 pp.

Nesbitt, S. W., E. J. Zipser, and D. J. Cecil, 2000: A census of precipitation features in the Tropics using TRMM: Radar, ice scattering, and lightning observations. *J. Climate,* **13,** 4087–4106.

Petersen, W. A., and S. A. Rutledge, 2001: Regional variability in tropical convection: Observations from TRMM. *J. Climate,* **14,** 3566–3586.

Petty, G. W., 1995: Frequencies and characteristics of global oceanic precipitation from shipboard present weather reports. *Bull. Amer. Meteor. Soc.,* **76,** 1593–1616.

Saunders, C. P. R., W. D. Keith, and R. P. Mitzeva, 1991: The influence of liquid water on thunderstorm charging. *J. Geophys. Res.,* **96,** 11 007–11 017.

Smith, E. A., A. Mugnai, H. J. Cooper, G. J. Tripoli, and X. Xiang, 1992: Foundations for statistical–physical precipitation retrieval from passive microwave satellite measurements. Part I: Brightness-temperature properties of a time-dependent cloud-radiation model. *J. Appl. Meteor.,* **31,** 506–531.

Spencer, R. W., 1986: A satellite passive 37-GHz scattering-based method for measuring oceanic rain rate. *J. Climate Appl. Meteor.,* **25,** 754–766.

——, H. M. Goodman, and R. E. Hood, 1989: Precipitation retrieval over land and ocean with the SSM/I: Identification and characteristics of the scattering signal. *J. Atmos. Oceanic Technol.,* **6,** 254–273.

Takahashi, T., 1978: Riming electrification as a charge generation mechanism in thunderstorms. *J. Atmos. Sci.,* **35,** 1536–1548.

——, 1983: A numerical simulation of winter cumulus electrification. Part I: Shallow cloud. *J. Atmos. Sci.,* **40,** 1257–1280.

——, 1984: Thunderstorm electrification—A numerical study. *J. Atmos. Sci.,* **41,** 2541–2558.

——, 1985: The role of liquid water on an ice surface during riming electrification—Basic experiment in thunderstorm electrification. *J. Meteor. Soc. Japan,* **63,** 262–266.

Takeuchi, T., M. Nakano, M. Brook, D. J. Raymond, and P. Krehbiel, 1978: The anomalous winter thunderstorm of the Hokuriku coast. *J. Geophys. Res.,* **83,** 2385–2394.

Toracinta, E. R., K. I. Mohr, E. J. Zipser, and R. E. Orville, 1996: A comparison of WSR-88D reflectivities, SSM/I brightness temperatures, and lightning for mesoscale convective systems in Texas. Part I: Radar reflectivity and lightning. *J. Appl. Meteor.,* **35,** 902–918.

——, D. J. Cecil, E. J. Zipser, and S. W. Nesbitt, 2002: Radar, passive microwave, and lightning characteristics of precipitation systems in the Tropics. *Mon. Wea. Rev.,* **130,** 802–824.

Vivekanandan, J., J. Turk, and V. N. Bringi, 1991: Ice water path estimation and characterization using passive microwave radiometry. *J. Appl. Meteor.,* **30,** 1407–1421.

Wilheit, T. T., 1986: Some comments on passive microwave measurement of rain. *Bull. Amer. Meteor. Soc.,* **67,** 1226–1232.

Wu, R., and J. A. Weinman, 1984: Microwave radiances from precipitating clouds containing aspherical ice, combined phase, and liquid hydrometeors. *J. Geophys. Res.,* **89,** 7170–7178.

Xie, P., and P. A. Arkin, 1997: Global precipitation: A 17-year monthly analysis based on gauge observations, satellite estimates, and numerical model outputs. *Bull. Amer. Meteor. Soc.,* **78,** 2539–2558.

Zipser, E. J., and K. R. Lutz, 1994: The vertical profile of radar reflectivity of convective cells: A strong indicator of storm intensity and lightning probability? *Mon. Wea. Rev.,* **122,** 1751–1759.